

Scientific paper

Brain Targeted Drug Delivery System of Carmustine: Design, Development, Characterization, *in vitro*, *ex vivo* Evaluation and *in vivo* Pharmacokinetic Study

Audumbar Mali o *,1 and Anil Bhanwase o 2

¹ School of Life Sciences, Punyashlok Ahilyadevi Holkar Solapur University, Solapur, 413255, Maharashtra, India.

² Department of Pharmaceutical Chemistry, SPM's College of Pharmacy, Akluj-413101, Malshiras, Solapur, Maharashtra, India.

* Corresponding author: E-mail: maliaudu442@gmail.com

Received: 09-20-2023

Abstract

The treatment of gliomas remains difficult task. Carmustine is a drug that is used in the treatment of gliomas. Flexible liposomes embedded *in situ* thermoreversible nasal gel preparations of Carmustine were studied for *in vitro* carmustine release, *ex vivo* carmustine permeation and carmustine release kinetics. The epithelial layers of nasal tissue were found to be intact and undamaged during histological analysis. Intranasal administration of optimized flexible liposomes embedded in a nasal gel showed higher C_{max} (Approximately two-fold), $AUC_{0\rightarrow t}$ (Approximately three-fold), $AUC_{0\rightarrow t}$ (Approximately six-fold), and lower T_{max} (1 h) in the brain, compared to intravenous injection of carmustine. The present study demonstrates that the flexible liposome embedded thermoreversible *in situ* intranasal gel of carmustine improved the targeted uptake of carmustine in the brain through the nasal delivery system and could be a reliable and effective delivery system for carmustine in the treatment of gliomas.

Keywords: Flexible liposomes, carmustine, zeta potential, AUC, C_{max} , T_{max} .

1. Introduction

Glioma is the most critical type of brain tumor among human beings. Patients suffering from glioblastoma (GBM) have survival period of 8–14 months. Surgery, chemotherapy, and radiation are the prevailing measures to treat GBM. Endothelial junctions of the blood-brain barrier (BBB) proved major challenge in the treatment of GBM. Many drug molecules are ineffective in clinical trials because of their inability to cross BBB. Oral route is not suitable to distribute the therapeutic amount of medication to the brain because of its specific obstacles, viz. BBB, blood-cerebrospinal fluid barrier, and efflux transporters. These obstacles regulate the exchange between the circulatory system for cerebrospinal fluid and peripheral blood flow. The administration of medicines into the central nervous system (CNS) seems more complicated due to other elements like physicochemical characteristics of the drug.^{1,2,3} Therefore variety of strategies are being used to target medicines to the brain, including BBB disruption, drug manipulation, as well as alternative routes of drug administration, viz. olfactory pathways (intranasal route), intrathecal, intra-cerebral, and ventricular. The nasal route

is a novel, useful, simple, and efficient way to cross the blood-brain barrier, which has led to its recent rise in popularity. It reduces systemic exposure and, consequently, systemic side effects related to medication use. The drug enters the CNS through the olfactory epithelium region due to the neuronal link between the nasal mucosa and the brain, which serves as a doorway for chemicals entering the central nervous system. ^{4,5,6}

Carmustine has been referred for the treatment of gliomas.^{7–10} However; it has been restricted because of side effects like bone marrow suppression¹¹ and pulmonary fibrosis.¹² Gliadel wafers¹³ are impregnated with carmustine and placed at the tumor site to lower side effects. These gliadel wafers are unsuccessful due to low tumor penetration, insufficiency to stop tumor recurrence, an absence of synergistic activity with other chemotherapeutic medicines including radiotherapeutic agents, and insufficient therapeutic efficacy.^{14,17} To overcome these glitches, an assortment of drug distribution vehicles has been developed in current days. This contains nanoparticles made of poly (D, L-lactic-co-glycolic) acid, polymeric micelles, liposomes, dendrimers, nanoshells, carbon nanotubes, polyglycolic acid, and polylactic acid.^{15,16,17} Despite several

study designs and research carried out, it is still a challenge to deliver required amount of carmustine to the brain.

The present work is designed to formulate Carmustine embedded flexible liposomal thermoreversible in situ intranasal gel for better brain targeting and effective therapeutic outcomes. The transdermal administration of flexible liposomes, viz. ethosomes, has produced some encouraging outcomes. 19-23 Researchers have proved the enhanced pharmacokinetic profiles for rizatriptan benzoate, salmon calcitonin, and galanthamine hydrobromide by transforming the drug into flexible liposomes. 24,25,26 Flexible liposomes have more bilayer elasticity because they lack cholesterol and have a higher amount of ethanol (20-40%) than typical liposomes, which are rigid because they contain cholesterol. Since intercellular pores are smaller than liposomes, the elasticity of liposomes expands penetration through them. By encouraging flux forces of the liposomes at middle-level concentrations, ethanol improves inter-vesicle repulsion and prevents aggregation. These flexible liposomes are, therefore, extra stable compared to regular liposomes. The flexible liposome penetrates the stratum corneum, and releases the medication in deepest layers of the skin. Topical application of flexible liposomes reaches therapeutic level in the plasma. Viscosity and mucoadhesive strength for different thermoreversible gels can be improved by extending the residence time in the intranasal cavity.^{27,28}

Vani et al., 2022 developed nano-sized carmustine liposomes with reasonable entrapment efficiency. ⁴² Hence, there is need to deliver carmustine effectively to the brain through appropriate drug delivery system.

2. Materials and Methods

Carmustine was obtained as gift sample from MSN Laboratories Private Limited, Telangana, India. Poloxamer 407 and Carbopol 934 were obtained as gift samples from BASF India Limited, Navi Mumbai, Maharashtra, India and Research Lab Fine Chem Industries, Mumbai, Maharashtra, India respectively.

2. 1. Compatibility Study of Excipients With Carmustine

The compatibility between selected excipients along carmustine was evaluated using an FTIR. FTIR spectra of carmustine with a physical blend of carmustine, lipids, polymers, and other excipients were scanned.²⁹

2. 2. Preparation and Characterization of Flexible Liposomes

Flexible liposomes were prepared by using ethanol injection method.^{26,30} Ethanol was mixed using a magnetic stirrer (2 MLH, 220/230 V AC supply, Bio Technics India) to dissolve the carmustine and soya lecithin. Using a sy-

ringe, double-distilled water was gradually added to the mixture as a thin stream (500 μ l /min), which made up to 30 ml, and the mixture was agitated for 30 minutes at 750 rpm with the help of a magnetic stirrer. To prevent ethanol loss, parafilm was used to cover the dispersion. Throughout the entire process, temperature was maintained at 30°C. The developed flexible liposomes were sonicated using a probe sonicator for three cycles of 5 minutes each, with 5 minutes of rest. The sonication was performed in an icy atmosphere to prevent an excessive rise in the temperature during the process. Formulation batches (F1–F9) were prepared by varying soya lecithin and ethanol ratio.

2. 3. Full Factorial Design for Preparation of Flexible Liposomes of Carmustine

The 3^2 full factorial designs were used in the current research work. In this research work, two factors were estimated, each at three different levels, and experimental trials were accomplished at all nine possible combinations. Particle size (Y_1) , percent entrapment efficiency (EE) (Y_2) , and polydispersity index (PDI) (Y_3) were used as dependent variables. In contrast, % of ethanol (X_1) and % of soya lecithin (X_2) in the final preparation were used as independent factors. The three levels for least, adequate, and extreme concentrations were classified as -1, 0, and +1, respectively, and presented in Tables in the supplementary material. Responses of different formulations were measured as per factorial design. 26,43

The responses were assessed using an interactive and polynomial statistical model.

$$Y = b_0 + b_1 X_1 + b_2 X_2 + b_{11} X_1^2 + b_{22} X_2^2 + b_{12} X_1 X_2$$

In the above equation, Y is the dependent variable, b_0 is the arithmetic mean response for nine runs, and b_i (b_1 , b_2 , b_{12} , b_{11} , and b_{22}) is the estimated coefficient of corresponding factors X_i (X_1 , X_2 , X_1X_2 , X_1^2 , and X_2^2). Critical effect (X_1 and X_2) signifies average results of changing 1 factor from its lower to higher values simultaneously.

The interaction term (X_1X_2) indicates how the response changes when two factors are changed concurrently. Polynomial terms X_1^2 and X_2^2 determine the quadratic impact. To analyze how independent variables impact dependent variables, the fit summary and analysis of variance (ANOVA) were combined to create the best-fit model. Design-expert software (Stat-Ease* 360) was used to optimize carmustine drug delivery system. 26,31,43

3. Characterization of Prepared Flexible Liposomes

3. 1. % Entrapment Efficiency (% EE)^{26,32}

The % EE of liposomal dispersions was determined by separating non-encapsulated carmustine from carmus-

tine liposome dispersion by centrifuging 2 ml of carmustine liposomes at 20000 rpm for 15 minutes at 4 °C. The supernatant layer was removed, sediment liposomes were disrupted with 2 ml ethanol to release entrapped Carmustine, then diluted using distilled water up to 10.00 ml and estimated for carmustine presence at 231 nm to calculate % EE by using a plotted calibration curve in phosphate buffer saline pH 6.4 (linearity, range = 0.50–2.50 μ g/ml, R^2 = 0.9996). The amount of carmustine entrapped was calculated:

% Entrapment Efficiency = $(W_a - W_s) / W_a \times 100$

Where,

 W_a is the total quantity of carmustine initially added W_s is the concentration of carmustine in liposomes.

3. 2. Carmustine Liposomes size, PDI, and Zeta Potential^{1,26}

The liposomal size for prepared flexible liposomes was assessed using the dynamic light scattering method and the Malvern Zeta sizer (ZSU3100, Nano ZS, Malvern Instruments Ltd., UK) particle size analyzer. The PDI was computed to examine liposomal size distribution. Malvern zeta sizer was used to calculate the zeta potential of each carmustine batch.

3. 3. Flexible Liposomes Surface Morphology and Shape^{1,18,26}

Surface morphology of liposomes was studied using Atomic Force Microscopy (AFM) and Transmission Electron Microscopy (TEM). For TEM examination, samples were mounted on carbon-coated grids, negatively stained using a phosphotungstic acid solution, and then observed under a microscope at 10,000–60,000 times the original magnification while accelerated at 100 kV. In the non-contact approach, silicon nitride cantilevers were used to investigate the Nanosurf Flex AFM model at room temperature.

3. 4. Embedded flexible liposomes in thermoreversible *in situ* gel

Stable liposomal dispersions (F1-F9) were converted into thermoreversible *in situ* gel formulations using a cold technique. Based on preliminary research, poloxamer 407 and carbopol 934 were used to transform the sol into gel under intranasal circumstances. 0.3% carbopol 934 was slowly mixed with distilled water using a stirrer. Then, 20 ml flexible liposome dispersion was mixed using a mechanical stirrer with a speed of one thousand revolutions per minute for thirty minutes to obtain the last mixture with Carmustine (0.2 mg/ml). Poloxamer 407 (18.00%) was mixed into the mixture. The prepared mixture was left

at 4 °C overnight to produce a clear solution. The viscosity, mucoadhesive strength, and other physicochemical properties of the gel were investigated. ^{26,33}

4. Evaluation Parameters

4. 1. Physico-chemical Characteristics of Carmustine Nasal Gel

The pH of intranasal gel, carmustine concentration, viscosity, and mucoadhesive strength were assessed. The pH of all batches was tested using a pH meter (Equip-Tronics EQ- 610). Carmustine content was determined with the help of a UV-visible spectrophotometer (Shimadzu 1800, Japan) at 231nm. At various temperatures (20 °C–40 °C), rheological investigations were carried out using a thermostatically precise Brookfield viscometer (DV3T Rheometer, USA). The mucoadhesive strength was assessed using a Texture Analyzer CT3 (Brookfield, USA) outfitted with a 4.5 kg load cell with Texture Pro CT software. 27,34,35,37

4. 2. Spreadability

The spreadability of nasal gel preparations was measured by using Whatman filter paper (#0.45 mm). Graduated pipette (1 ml) with a rubber bulb was clamped vertically to stand where its tip was kept 2 cm above the horizontal surface of round filter paper. At the center of the filter paper, 0.1 ml of the gel preparation was dropped. At a fixed time interval of 20 seconds, the surface area covered by gel was observed and evaluated.³⁶

4. 3. In vitro Carmustine Release Studies

In vitro drug release study was performed by using Franz diffusion cell. Cellophane membrane (molecular weight: – 12,000.00–14,000.00) having a permeation area of 0.8 cm² was used for permeation study. 15 ml of Phosphate Buffer Saline (pH 6.4) was retained in the receptor chamber, and carmustine nasal gel containing a carmustine equivalent to 1mg was retained in the donor chamber. A 0.5 ml sample was taken from the receptor compartment at predetermined intervals by continuously replacing it with freshly prepared buffer solution for eight hours. Then, samples were diluted and estimated for carmustine content with the help of UV spectrophotometer at 231nm. ^{37,38,39}

4. 4. Ex-vivo Carmustine Release Study for Carmustine in situ Nasal Gel

The freshly isolated nasal cavity of the sacrificed goat was taken from the local slaughterhouse, and kept in Phosphate buffer saline (pH 6.4). Mucosal membrane was identified, removed, cleaned, and maintained in Phosphate buffer saline. A Franz diffusion cell with a thermo-

stat facility was used to conduct the study. Franz diffusion cells with an actual permeation component of 2.00×2.00 cm² were used to hold tissue sections. Carmustine-loaded thermoreversible nasal gel equivalent to 1 mg of carmustine was kept in the donor compartment, and the receptor compartment was filled using 15 ml of Phosphate buffer saline (pH 6.4). The study was carried out at 34 ± 1 °C under stirring. Aliquots of 0.5 ml were taken from the receptor compartment and substituted for 8 hours using a new buffer. The samples were diluted before being examined with a UV spectrophotometer at 231 nm. 37,38,39

4. 5. Release Kinetics of Carmustine

All preparations of carmustine were taken to study release kinetics. The release profile was evaluated for best fit model. 40

4. 6. Histopathological Study Using Nasal Mucosa

Histopathological evaluation of nasal mucosa was carried out after *ex-vivo* permeation study. The nasal membrane was set aside on the glass slide with the help of a 10% buffered formaldehyde solution. Nasal tissue parts were colored by using hematoxylin with eosin, and then finally seen by using a light microscope to check for signs of tissue damage caused during *ex-vivo* drug permeation.¹⁰

4. 7. In Vivo Pharmacokinetic Study

Healthy Wistar rats of 3 to 4 months, weighing 200–250 grams were included in study. The rats were kept in a neat and hygienic room at 25 ± 1 °C along with humidity of 45–55%, for 12 hrs /12 hrs light and dark conditions. The rats have given free access to food and water. The Ethical clearance (CPCSEA/IAEC/CP-PL/01/2023) was obtained from Institutional Animal Ethics Committee (IAEC) of Sudhakarrao Naik Institute of Pharmacy, Yavatmal, Maharashtra, India. The rats were fasted the whole night before the work. Rats were divided in five different groups comprising three animals in each group. 46,47

4. 8. In Vivo Pharmacokinetic Study in Brain

All rats were kept at 25 \pm 1 °C and fasting overnight. Two groups of rats are as follows:

Group 1 – Intranasal administered optimized flexible liposome embedded *in situ* thermoreversible nasal gel.
 Group 2 – The Carmustine-marketed formulation, (Carmustine for injection USP 100 mg) was administered IV through the tail vein.

 $20 \mu l$ of gel containing carmustine (0.81 mg/kg) was applied to nostrils of each animal in the first group, 42 and,

marketed carmustine injection was given to each animal in the second group through the tail vein, which containing carmustine corresponding to 0.81 mg/kg. The rats stayed supine for two minutes after taking carmustine preparations. Rats were sacrificed using intraperitoneal urethane (1g/kg). The brain was isolated at different time intervals, viz. 15 minutes, 30 minutes, 1 hour, 2 hours, 4 hours, 6 hours, and 8 hours. Brain samples were homogenized in methanol and mixed with acetonitrile. Homogenate was filtered and examined using HPLC.⁴⁸

4. 9. Statistical Examination

PK Solver software was used for statistical analysis.

5. Results

5. 1. Compatibility Study of Excipients with Carmustine

The drug-excipient compatibility was assessed using an FTIR spectrophotometer. The infrared spectrum of carmustine and physical mixture of carmustine with excipients were compared (Figure 1). No variations were observed in the spectrum of carmustine. This indicates that carmustine is compatible with a mixture of excipients. The distinctive peaks of the carmustine FTIR spectrum may correspond to secondary amine groups at 3331 cm⁻¹ and to the C=O stretch at 1708 cm⁻¹. In addition, peaks at 1380 cm⁻¹, and 2973 cm⁻¹ for N=O and aliphatic C-H stretch were observed respectively. The C-O stretch was observed at 1087 cm⁻¹ and 1045 cm⁻¹, C-X (chloride) was observed at 803.78 cm⁻¹ and 654 cm⁻¹ respectively C-N stretch (amines) was observed at 1274 cm⁻¹ and 1329 cm⁻¹ respectively. Typical characteristic peaks of the carmustine were also seen in the FTIR spectrum of the physical mixture with no noticeable change from the spectra of the separate carmustine and excipients. This demonstrated that carmustine and excipients did not interact chemically.41

5. 2. Evaluation for Carmustine Flexible- Liposomes

Carmustine flexible liposomes were prepared by using an ethanol injection sonication method. Probe sonication causes a cavitation effect, where sonic vibrations are translated into dispersion, which forms several tiny bubbles. The internal pressure of system is raised due to these tiny bubbles leading collision of particles and reduction of their size to nanoscale. Carmustine flexible liposomes were stored at cold temperature (2–8 °C) for further study.

Table 1 depicts the liposomal particle size, % of EE, PDI, and zeta potential.

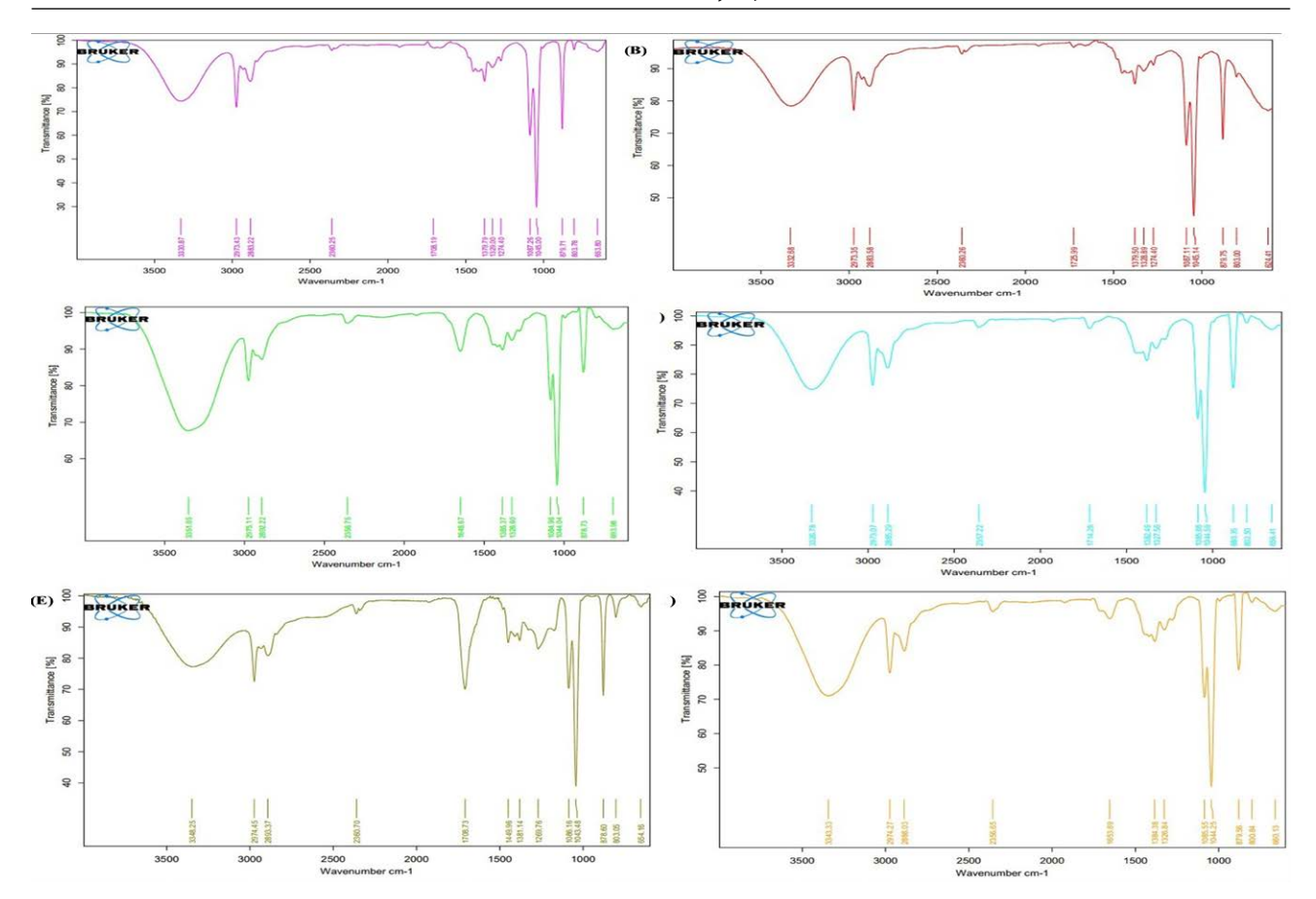


Figure 1. (A) FTIR spectrum of Carmustine API in Ethanol (Carmustine solution), (B) FTIR spectrum of Carmustine solution + Soya Lecithin, (C) FTIR spectrum of Carmustine solution + Soya Lecithin + water, (D) FTIR spectrum of Carmustine solution + Poloxamer 407, (E) FTIR spectrum of Carmustine solution + Carbopol 934, (F) FTIR spectrum of Carmustine + All excipients

Table 1. Characterization of flexible liposomes

Batches code	Coded values		Particle Size	Entrapment Efficiency	PDI Y ₃	Zeta Potential
	Ethanol (%) X ₁	Soya Lecithin (%) X ₂	(nm) Y ₁	(%)Y ₂	J	(mV)
F1	-1	-1	146.8 ± 10.2	96.9± 1.2	0.1	-28.3 ± 4.2
F2	-1	0	149.8 ± 16.0	94.9± 1.1	0.2	-50.2 ± 4.8
F3	-1	+1	180.3 ± 10.2	94.4 ± 1.7	0.2	-20.3 ± 2.9
F4	0	-1	181.1 ± 14.3	98.6± 1.1	0.3	-47.8 ± 3.5
F5	0	0	180.5 ± 21.4	96.9± 1.2	0.2	-26.2 ± 4.9
F6	0	+1	197.7 ± 14.1	96.9 ± 1.2	0.4	-24.0 ± 5.2
F7	+1	-1	187.8 ± 20.2	91.9± 1.1	0.4	-67.5 ± 6.2
F8	+1	0	180.5 ± 18.7	92.2± 1.6	0.4	-48.7 ± 4.7
F9	+1	+1	192.3 ± 12.9	91.0 ± 1.4	0.4	-39.4 ± 5.9

Note: $(n = 3, mean \pm Standard Deviation (SD))$

Where: Independent Variables = X1 - % of ethanol, X2 - % of soya lecithin, Dependent Variables = Y1 - Particle size (nm), Y2 - Percentage EE, Y3 - PDI.

5. 3. 3² Full Factorial Designs for the Formulation of Flexible Liposomes

A 3^2 full factorial design was applied to study the effect of factors systematically. With the help of Design Expert* software (Stat-Ease* 360), the impact of independent variables such as % Ethanol (X_1) and % Soya Lecithin (X_2)

was examined by contour plots and response surface plots by application of ANOVA (Table 1).

The following equations were formed via regression along with a graphical examination of results obtained in experimental values, where F ratios were statistically significant (p < 0.05), and Adjusted-R² values reached from 0.9880 to 0.9327. The results were well-fit by these model equations.

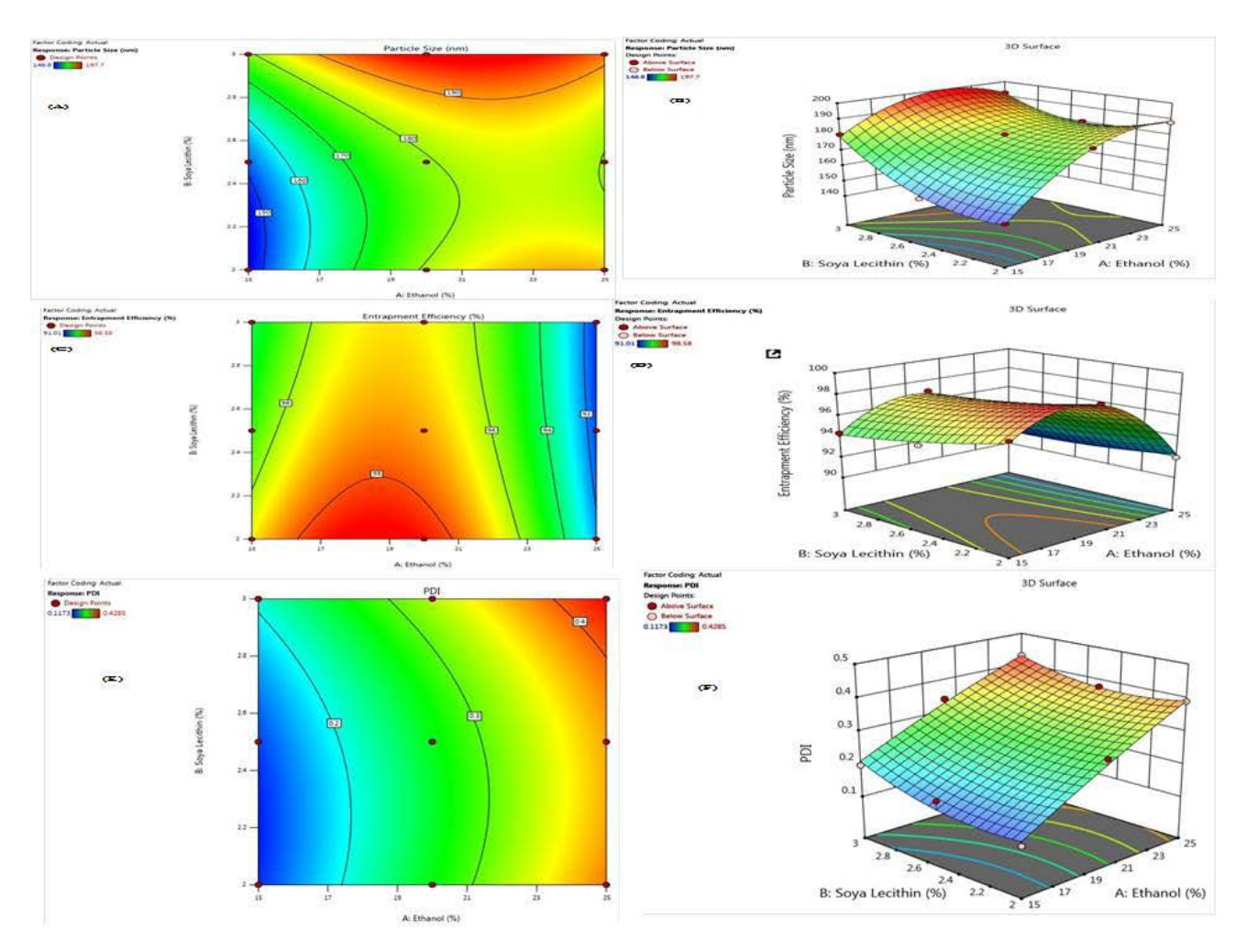


Figure 2. Contour plots (A, C, E) and Surface response plots (B, D, F) for particle size, % EE, and PDI respectively.

The impact on particle size (Y_1) , % EE (Y_2) , and PDI (Y_3) were observed to be significant by ANOVA, and the quadratic equation as below:

$$Y_1 = 1167.61X_1 + 496.86X_2 + 365.40X_1^2 + 230.41X_2^2 + 210.25X_1X_2$$
 (1)

$$Y_2 = 20.42X_1 + 4.49X_2 + 31.23X_1^2 + 0.1780X_2^2 + 0.6806X_1X_2$$
 (2)

$$Y_3 = 0.0865X_1 + 0.0050X_2 + 0.0002X_1^2 + 0.0021X_2^2 + 0.0004X_1X_2$$
 (3)

Flexible liposomes are seen in TEM photomicrographs to be unilamellar and almost spherical. The flexible liposomes deviate from the typical spherical shape of conventional liposomes due to lack of cholesterol. Cholesterol makes the liposomal bilayer dispersion rigid, its absence and a higher alcohol concentration make it flexible and cause it to deviate from the typical spherical shape. These observations are consistent with the earlier findings by Touitou *et al.*³⁰ and Kempwade *et al.*²⁶ Figure 3 depicts a TEM image of camustine flexible liposomes.

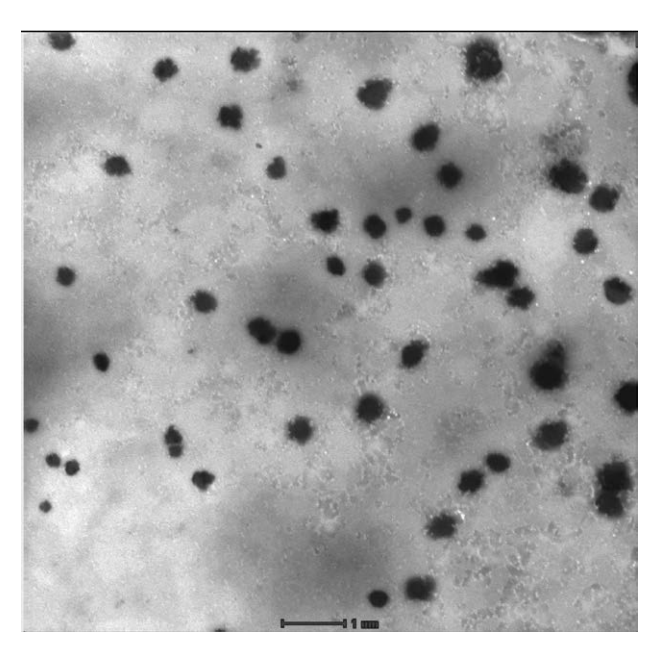


Figure 3. TEM results of carmustine flexible liposomes

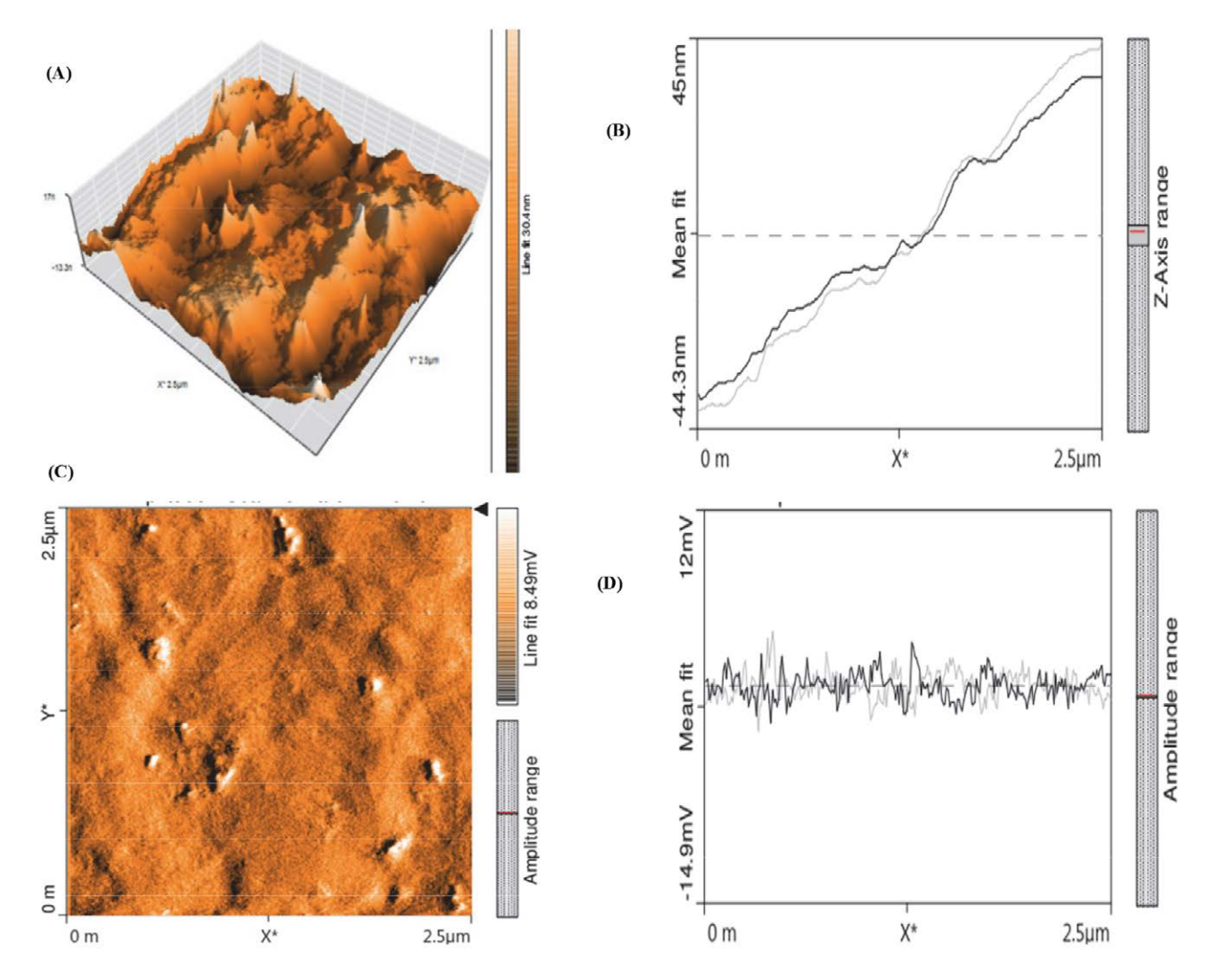


Figure 4 depicts AFM pictures of flexible liposomes. Flexible liposomes of carmustine underwent an AFM examination to evaluate their surface topography and size. Uniformly distributed, roughly spherical-shaped liposomes can be seen in the AFM pictures.

The physicochemical properties of the produced flexible liposomes implanted in *in situ* nasal gels were evaluated. It was seen that the gelation time was less than 15 seconds. The gel developed right away as the temperature reached 32 to 34 °C. It was observed that the mucoadhesive strength was 3726.52 to 4667.96 dynes/ cm². The formulation's viscosities ranged from 6579 \pm 49.90 cps to 7032 \pm 80.62 at 30 °C \pm 1 °C. The pH of optimized formulations was observed from 5.50 \pm 0.38 to 6.02 \pm 0.58. The % carmustine content of optimized *in situ* nasal gel preparations was 97.00 \pm 2.18 to 99.34 \pm 1.97. The spreadability of optimized formulations was observed from 16.28 \pm 2.05 to 18.75 \pm 1.89.

5. 4. *In vitro* Carmustine Release Study

Flexible liposomes embedded in situ nasal gel is required to release drug slowly for longer time. Therefore, these formulations of carmustine were studied for release kinetics by performing an *in vitro* drug release study for

eight hours. Samples were withdrawn at intervals of 15 minutes, 30 minutes, one hour, two hours, four hours, six hours, and eight hours. In nine different formulations, the TG7 formulation showed the lowest cumulative % drug release, observed to be 83.7%, whereas TG4 showed the highest cumulative % drug release, observed to be 96.2% (Figure 5 A). The comparative *in vitro* release profile of carmustine API solution, flexible liposomes of carmustine, *in situ* nasal gel of carmustine, and flexible liposomes embedded *in situ* nasal gel of carmustine followed zero order kinetics. Carmustine API solution showed lowest cumulative % drug release which was observed to be 56.2%. However; flexible liposomes embedded *in situ* nasal gel showed the highest cumulative % drug release which was observed to be 96.1% (Figure 5 B).

5. 5. Ex-vivo Carmustine Permeation Study

Ex-vivo carmustine permeation study was performed using a nasal membrane. Drug permeation was

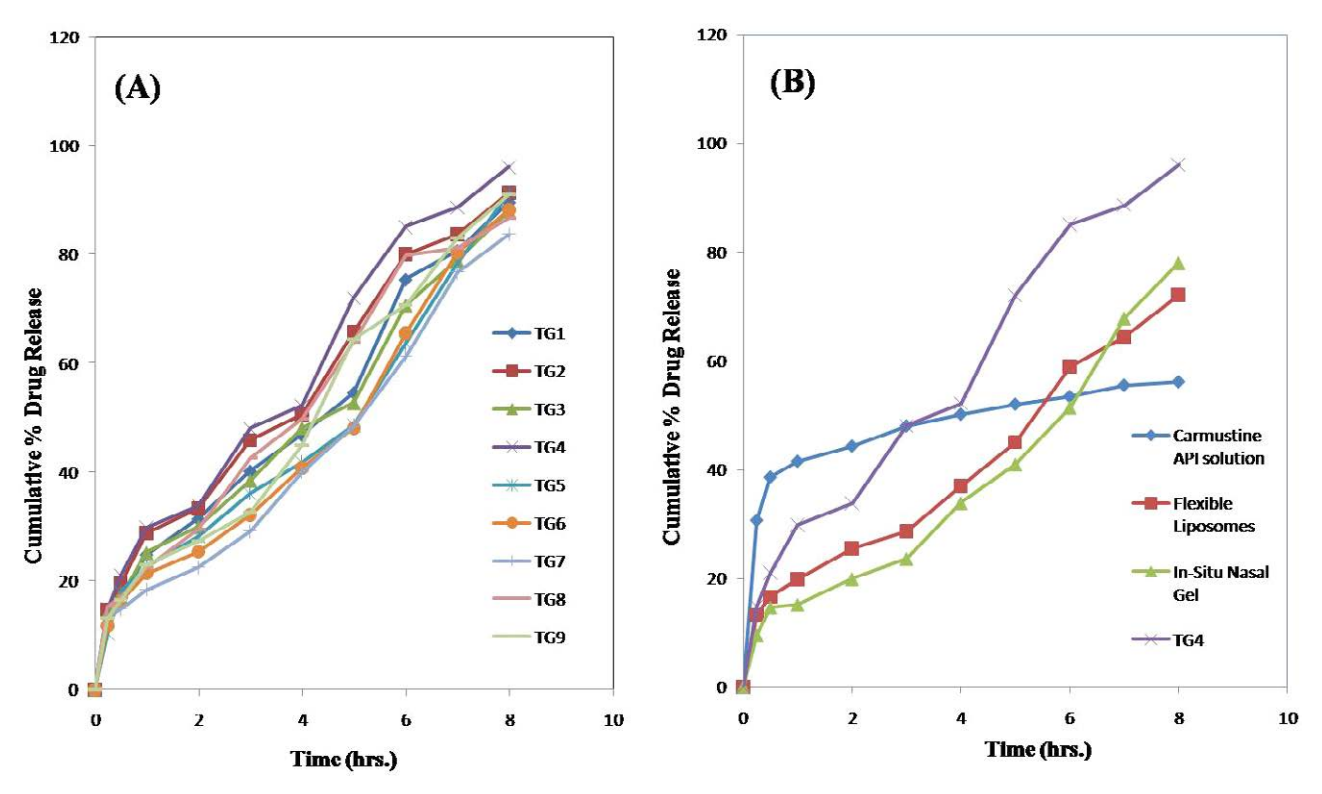


Figure 5. (A) % Cumulative drug release of flexible liposomes embedded *in situ* in thermoreversible nasal gel (TG1-TG9), (B) % Cumulative drug release of Carmustine API solution, flexible liposomes, *in situ* nasal gel of carmustine and TG4

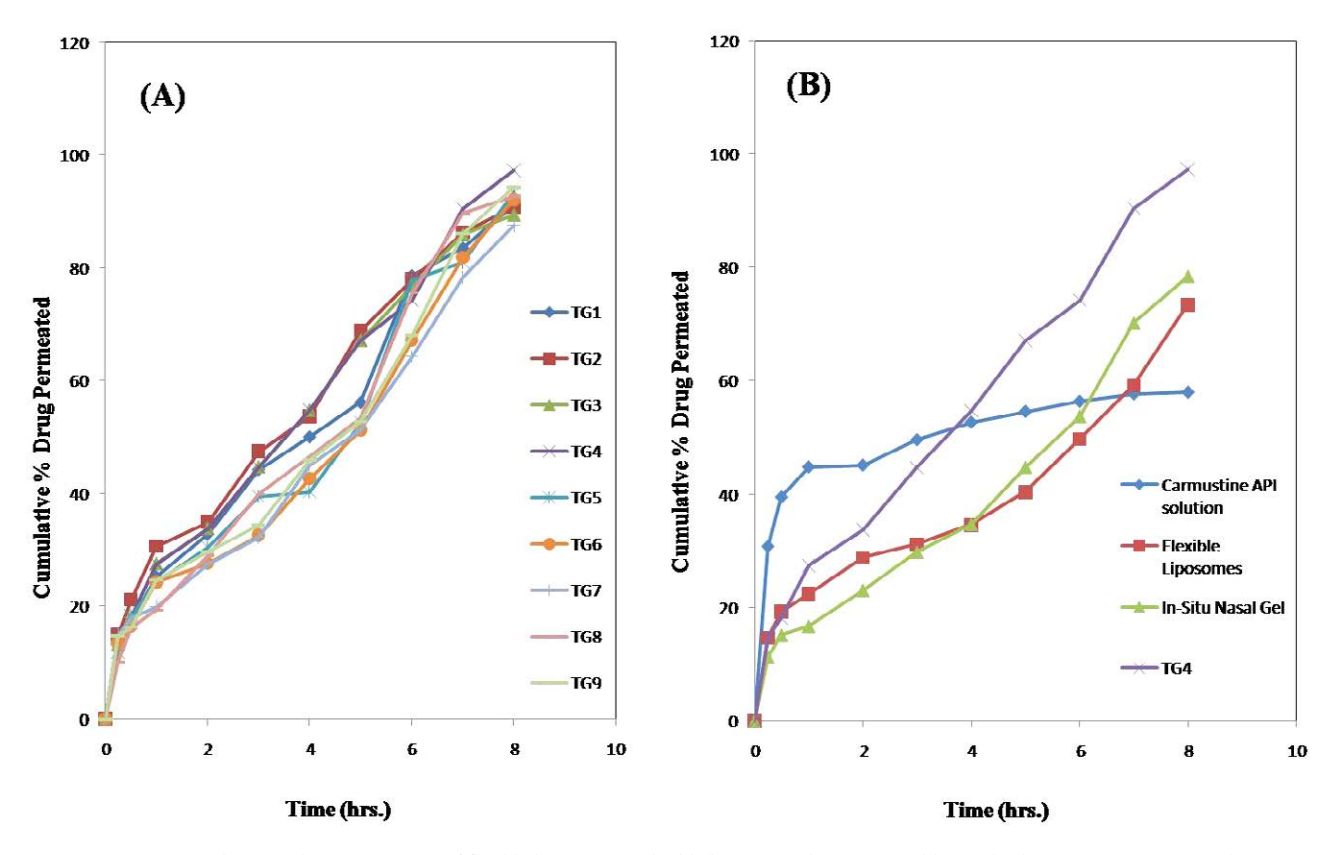


Figure 6. (A) Cumulative % drug permeation of flexible liposomes embedded *in situ* in thermoreversible nasal gel (TG1-TG9), (B) Cumulative % drug permeation of Carmustine API solution, flexible liposomes, *in situ* nasal gel of carmustine and TG4

assessed for eight hours at specified time intervals. Maximum drug permeation was observed in case of TG4; however, TG7 showed minimum drug permeation across the goat nasal membrane. In nine different formulations, the TG7 formulation showed the lowest drug permeation, observed to be 87.5%, whereas TG4 showed the highest drug permeation, observed to be 97.4% (Figure 6 A).

Comparative *ex-vivo* permeation of the carmustine across goat nasal membrane for TG4 with other formulations viz. carmustine API solution, flexible liposomes, and *in situ* nasal gel of carmustine followed zero order kinetics. TG4 showed the highest drug permeation (97.4%) and carmustine API solution showed the lowest drug permeation (58.1%) through the nasal membrane. (Figure 6 B).

5. 6. Determination of Carmustine Release Kinetics

Dissolution profile of different carmustine formulations were compared by using model dependent (Curve fitting) methods followed by statistical analysis. Higuchi's equation was the best-fit model as $r^2 = 0.9848$ for the *in vitro* carmustine release profile; zero-order and higuchi matrix kinetics were the best-fit models as $r^2 = 0.9912$ for *ex-vivo* carmustine release profile (Table 2).

The flux values of different flexible liposomes embedded *in situ* nasal gel formulations were obtained from 1.6119 (μ g/cm) 2 /min to 1.8491 (μ g/cm) 2 /min, and enhancement ratios for various formulations were obtained from 2.1483 to 2.4644. TG7 showed lowest flux value, whereas TG8 showed highest flux value. TG7 showed lowest enhancement ratio, whereas TG8 showed highest enhancement ratio.

5. 7. Histopathological Study of Nasal Mucosa

Histopathological analysis was performed to verify cellular damage to goat nasal mucosa after an *ex-vivo* study. Nasal goat mucosa retained in phosphate buffer saline (SPBS) having pH 6.4 was a standard control. Pseudostratified columnar ciliated epithelium and lamina propria with mucus acini were normal. The epithelium layer of normal goat nasal tissue and tissue used for the perme-

ation study of carmustine was observed to be intact and without cellular damage Figures 7(A) and 7(B).

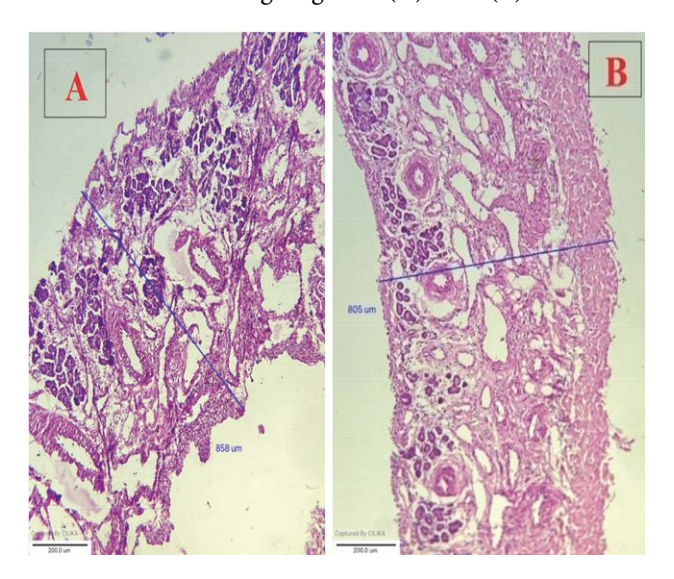


Figure 7. Histopathological study of goat mucosal membrane: (A) Nasal mucosal membrane kept in SPBS having pH 6.4, and (B) Nasal mucosal membrane used for permeation of TG4

5. 8. *In vivo* Pharmacokinetic Study

The drug concentration – time profile of carmustine flexible liposomes embedded *in situ* thermoreversible nasal gel (TG4) and marketed formulation is illustrated in Figure 8, Table 3.

It was observed that, absorption via nasal route of optimized flexible liposomes embedded *in situ* thermoreversible intranasal gel appears to be fast, along with more concentration of carmustine accomplishment in the brain within 0.25 h (55.1 % release), as compared to marketed intravenous drug delivery system (11.73 % release). The fact that the $T_{\rm max}$ following intranasal formulations was shorter (1 h) than that following IV administration (2 h) (Table 3) suggests that carmustine is rapidly transported to the brain through the nose. Nasal administration for TG4 observed approx. 2-fold higher $C_{\rm max}$ value in the nasal route than the IV route of the marketed formulation of carmustine injection (Table 3).

Table 2. Drug release kinetic models for optimized flexible liposomes embedded in situ nasal gel of carmustine

For <i>In vitro</i> drug release							
Formulations	Zero Order	First Order	Higuchi Matrix Kinetics	Korsmeyer Peppas Kinetics	Hixson-Crowell Model.	Best fit model	
TG4	0.9848	0.8525	0.9848	0.9564	0.9271	Higuchi Matrix Kinetics	
			For Ex-vivo dr	ug release			
TG4	0.9912	0.7767	0.9912	0.9789	0.8916	Zero Order & Higuch Matrix Kinetics	

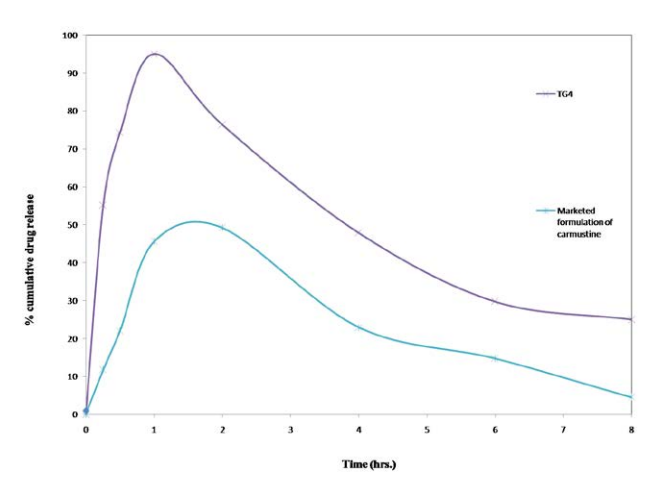


Figure 8. Drug concentration in brain time profile of carmustine formulation (TG4) and marketed formulation in rats

layer solubilization and serves to change the morphological characteristics of carmustine embedded liposomes. Another cause might be the rise in inter-vesicle repulsion with rise in intermediate ethanol amount by helping fluctuation force. More amount of ethanol affects liposomal fusion (due to too robust fluctuations or bilayer partial or local solubilization). Similar outcomes for several researchers have previously been observed. A4, 45 The amount of ethanol was similarly correlated with a slight but substantial decrease in percent entrapment efficiency (p < 0.05).

The adjusted determination coefficient ($R^2 = 0.9880$, 0.9558, and 0.9327 for Y_1 , Y_2 , and Y_3) and predicted determination coefficient ($R^2 = 0.9516$, 0.8179, and 0.9077 for Y_1 , Y_2 , and Y_3) results were comparative and give higher significance of the model.

Table 3. Pharmacokinetic parameters obtained from drug concentration in brain-time profile curve in Wistar rats.

Sr. No.	Formulations	Route of Administration	C _{max} (µg/ml)	T _{max} (h)	$AUC_{0 o t} (\mu g/h/ml)$	$AUC_{0\to\infty}(\mu g/h/ml)$	
01	TG4	Nasal	7.60 ± 0.49	1	1.38±0.20	14.65±0.25	
02	Marketed Formulation	n Intravenous	3.93 ± 0.36	2	0.45 ± 0.21	2.46 ± 0.24	
	(Carmustine for injection USP 100 MG)						

The bioavailability of TG4 optimized formulation through nasal delivery was observed to be higher approx.6.0 folds more than the marketed formulation of carmustine injection through the IV route (Table 3). This might be because of poor transport of the carmustine via the BBB. 48,49 A relative relationship of bioavailability of TG4 quantified through AUC $_{0\rightarrow t}$, indicated 3-fold more in the brain than the marketed formulation of carmustine injection (Table 3). Hence, it shows the potential ability and practical suitability of TG4 for effective delivery of carmustine to brain. In general, the pharmacokinetic parameters for intranasal administration of the TG4 nasal gel proved significant enhancement in the brain bioavailability of carmustine as compared to commercial IV injection of carmustine through the IV route.

6. Discussion

FTIR spectra of carmustine did not show any distinctive alteration when mixed with different ingredients like soya lecithin, and polymers. This indicates retention of structural and chemical integrity of the Carmustine after mixing all excipients.

Ethanol and soya lecithin, at varying amounts; give a positive association concerning the particle size of carmustine-embedded liposomes. The results revealed that ethanol is responsible for carmustine liposome size, PDI, and zeta potential with % EE. The liposomal size was increased with the increase in amount of ethanol. This may be because of the high ethanol amount, which affects bi-

By rejecting the null hypothesis, "P" values of 0.05 showed a significant interaction between selected independent variables.

For Y_1 , the model F-value of 132.81 shows that the model is significant. In this study, ethanol, soya lecithin, interaction terms, and polynomial terms significantly impact the particle size of liposomes.

The Y2 model's F-value of 35.62 shows that the model is significant. In this study, ethanol, soya lecithin, and polynomial terms significantly impact % entrapment efficiency.

The Y3 model's F-value of 56.46 shows that the model is significant. Only ethanol significantly impacts PDI in this study.

The "P" values for particle size, percentage entrapment efficiency, and PDI were 0.0010, 0.0071, and 0.0109, respectively. For 3^2 factorial design models, the sum of "P" and the adjusted R^2 values shows a substantial synergistic association between both independent variables at P < 0.05.

TG7 showed the lowest cumulative percentage of drug release (83.676%). TG4 showed the highest cumulative percentage of drug release; however, the carmustine API solution showed the lowest cumulative percentage drug release. In the *ex-vivo* carmustine permeation study, maximum drug permeation was observed in the case of TG4; however, TG7 showed minimum drug permeation across the goat nasal mucosa. TG4 showed the highest drug permeation, and carmustine API solution showed the lowest carmustine permeation across goat nasal mucosa From the *in vitro* dissolution and *ex-vivo* Carmustine permeation study, it was observed that the final optimized

TG4 preparation showed maximum cumulative % Carmustine release and maximum Carmustine permeation.

Histopathological study revealed that the intranasal administration of flexible liposomes embedded thermoreversible gel is safe. 42

The crucial target of the current work was to increase brain bioavailability of carmustine optimizing flexible liposomes embedded in situ nasal gel formulation. The BBB may diverge drug concentration-time profile in the brain significantly. Medicines in the brain are distributed and eliminated through various mechanisms, including diffusion, bulk flow of cerebrospinal fluid, extracellular-intracellular exchange, brain extracellular fluid, and metabolism in brain tissue. To predict the desired therapeutic effect, it is crucial to establish a link between the medicine-distribution processes throughout the brain, and the amount of the medicine in the brain. The outcome of a medicine that targets the brain could be reliably predicted by mathematical models depicting medicine transport via the brain capillary system, medicine transport over BBB, intra-extracellular interchange, medicine binding inside the brain, and medicine metabolism in the brain. 48,50,51 TG4 showed higher permeation of carmustine with higher C_{max}. Pharmacokinetic studies showed the importance of the nasal route administration of carmustine and significance of the TG4 to deliver carmustine effectively to brain.

7. Conclusion

Intranasal route of drug administration is considered as an effective methodology for transporting the therapeutic agents to the brain in managing brain tumors. Carmustine-embedded flexible liposomes-based *in situ* nasal gel formulations were developed and optimized. TG4 nasal gel of carmustine can improve carmustine delivery to the brain by increasing gel retention in the nasal membrane, and therefore increasing carmustine transport. Hence, in the current study, the TG4 was formulated, and assessed for its brain-targeting potential. The *in vivo* pharmacokinetics of TG4 showed more amount of carmustine is delivered to brain via nasal route. TG4 was proven to be safe for nasal mucosal tissue, and would be a safe, reliable, and convenient method of treating GBM.

List of abbreviations

TEM: - Transmission electron microscopy

AFM: - Atomic Force Microscopy

GBM: - Glioblastoma

BBB: - Blood-Brain Barrier

CNS: - Central Nervous System

FTIR: - Fourier Transform Infrared Spectrophotometer

PDI: - Polydispersity Index

SD: - Standard Deviation

SPBS: - Saline Phosphate Buffer Solution

IV: - Intravenous

Author contribution statement

Each mentioned contributor contributed substantially to this manuscript's idea and writing.

Declarations

Conflict of Interest

The authors declare that they have no conflict of interest.

8. Acknowledgement

The authors thank MSN Laboratories Private Limited, Telangana, and BASF India Limited, Navi Mumbai, Maharashtra, for providing gift samples of Carmustine and Poloxamer 407, respectively. The authors are grateful to the School of Life Sciences, PAH Solapur University, Solapur; Sahyadri College of Pharmacy, Methwade, Sangola, Solapur and Shikshan Prasarak Mandal's College of Pharmacy, Akluj, Malshiras, Solapur, Maharashtra for providing all facilities to complete this work.

9. References

- M. Alagusunda, K. B. Chandra Sekhar, G. Nethra Vani, J. Med. Pharma. Allied Sci. 2022, 11, 4518–4526.
 DOI:10.55522/jmpas.V11I2.2159
- 06/03/2022. https://www.healthline.com/health/brain-cancer#treatments
- 3. 17/03/2022. https://www.healthline.com/health/brain-tu-mor#types
- L. Illum, Drug Disc. Today. 2002, 7, 1184–1189.
 DOI:10.1016/S1359-6446(02)02529-1
- A. K. Mitra, R. Krishnamoorthy, *Adv. Drug Deliv. Rev.* 1998, 29, 135–146. DOI:10.1016/S0169-409X(97)00065-3
- S. Khan, K. Patil, N. Bobade, J. Drug Target. 2010, 18, 223– 234.

DOI:10.3109/10611860903386938

- B. S. Satapathy, J. Panda, *Int. J. App. Pharm.* 2020, *12*, 240–248. DOI:10.22159/ijap.2020v12i5.37885
- 8. R. B. Weiss, B. F. Issell, *Can. Treat. Rev.* **1982**, *9*, 313–330. **DOI:**10.1016/S0305-7372(82)80043-1
- M. I. Alam, S. Beg, A. Samad, Eur. J. Pharm. Sci. 2010, 40, 385–403. DOI:10.1016/j.ejps.2010.05.003
- A. R. Khan, M. Liu, M. W. Khan, J. Cont. Rel. 2017, 28, 364–389. DOI:10.1016/j.jconrel.2017.09.001
- 11. V. Bourganis, O. Kammona, A. Alexopoulos, *Eur. J. Pharm. Biopharm.* **2018**, *128*, 337–362.

DOI:10.1016/j.ejpb.2018.05.009

- B. K. Driscoll, S. Kalra, H. R. Gattamaneni, Chest. 1995, 107, 1355–1357. DOI:10.1378/chest.107.5.1355
- S. H. Lin, L. R. Kleinberg. Exp. Rev. Antican. Ther. 2008, 8, 343–359. DOI:10.1586/14737140.8.3.343
- 14. E. Muntimadugu, R. Dhommati, A. Jain, *Eur. J. Pharm. Sci.* **2016**, *20*, 224–234. **DOI:**10.1016/j.ejps.2016.05.012

- A. Prokop, J. M. Davidson, J. Pharma. Sci. 2008, 97, 3518–3590. DOI:10.1002/jps.21270
- G. Invernici, S. Cristini, G. Alessandri, Rec. Pat. Antican. Drug Discov. 2011, 6, 58–69. DOI:10.2174/157489211793979990
- Y. Shufeng, F. Yang, C. Jie, G. Zhang, Arti. Cel. Nano and Biotech. 2019, 47, 3438–3447.
 - DOI:10.1080/21691401.2019.1652628
- M. K. Chourasia, L. Kang, S. Y. Chan, Res. Pharma. Sci. 2011, 1, 60–67. DOI:10.1016/j.rinphs.2011.10.002
- G. Li, Y. Fan, C. Fan, X. Li, X. Wang, M. Li, Eur. J. Pharm. Biopharm. 2012, 82, 49–57. DOI:10.1016/j.eipb.2012.05.011
- R. G. Maheshwari, R. K. Tekade, P. A. Sharma, G. Darwhekar,
 A. Tyagi, R. P. Patel, *Saudi Pharm. J.* 2012, 20, 161–170.
 DOI:10.1016/j.jsps.2011.10.001
- 21. P. Verma, K. Pathak, *Nanomedicine*. **2012**, *8*, 489–496. **DOI:**10.1016/j.nano.2011.07.004
- K. Arumugam, G. S. Subramanian, S. R. Mallayasamy, R. K. Averineni, M. S. Reddy, N. Udupa, *Acta Pharm.* 2008, 58, 287–297. DOI:10.2478/v10007-008-0014-3
- S. P. Vyas, S. K. Goswami, R. Singh, *Int. J. Pharm.* 1995, 118, 23–30. DOI:10.1016/0378-5173(94)00296-H
- W. Li, Y. Zhou, N. Zhao, B. Hao, X. Wang, P. Kong, *Environ. Toxicol. Pharmacol.* 2012, 34, 272–279.
 DOI:10.1016/j.etap.2012.04.012
- M. Chen, X. R. Li, Y. X. Zhou, K. W. Yang, X. W. Chen, Q. Deng, *Peptides*. 2009, 30, 1288–1295.
 DOI:10.1016/j.peptides.2009.03.018
- A. A. Kempwade, A. D. Taranalli, R. D. Hiremath, S. A. Joshi, *Ind. J. Pharm. Sci.* 2022, 84, 863–873.
 DOI:10.36468/pharmaceutical-sciences.981
- 27. R. J. Majithiya, P. K. Ghosh, M. L. Umrethia, R. S. Murthy, *AAPS Pharm. Sci. Tech.* **2006**, *7*, E80-E86.
 - **DOI:**10.1208/pt070367
- 28. A. Agrawal, R. K. Maheshwari, *Asian J. Pharm.* **2011**, *5*, 131–140. **DOI:**10.4103/0973-8398.91988
- M. Yasir, U. Singh, I. Chauhan, Artificial Cells Nanomedi. and Biotech. 2018, 46, 1838–1851.
 DOI:10.1080/21691401.2017.1394872
- E. Touitou, N. Dayan, L. Bergelson, B. Godin, M. Eliaz, J. Cont. Rel. 2016, 65, 403–418.
 - **DOI:**10.1016/S0168-3659(99)00222-9
- B. Sudhakar, M. Krishna, K. Murthy, *Appl. Nanosci.* 2016, 6, 43–60. DOI:10.1007/s13204-015-0408-8
- 32. R. Fugate, N. Shivappa, S. R. Hyam, *J. Comp. Medi. Res.* **2021**, *12*, 7–20. **DOI**:10.5455/jcmr.2021.12.04.02
- A. Kempwade, A. Taranalli, J. Sol-Gel Sci. Tech. 2014, 72, 43–48. DOI:10.1007/s10971-014-3422-5
- 34. M. J. Bhandwalkar, A. M. Avachat, *AAPS Pharm. Sci. Tech.* **2013**, *14*, 101–110. **DOI**:10.1208/s12249-012-9893-1
- 35. U. C. Galgatte, A. B. Kumbhar, P. D. Chaudhari, *Drug Deliv.* **2014**, *21*, 62–73. **DOI:**10.3109/10717544.2013.849778
- S. Shelke, S. Shahi, S. Jalalpure, D. Dhamecha, S. Shengule, *J. Drug Del. Sci. Tech.* 2015, 29, 238–244.
 DOI:10.1016/j.jddst.2015.08.003
- D. M. Abouhussein, A. Khattab, N. A. Bayoumi, A. F. Mahmoud, T. M. Sakr, *J. Drug Del. Sci. Tech.* 2018, 43, 129–

- 140. **DOI:**10.1016/j.jddst.2017.09.021
- 38. M. V. Kumar, A. S. Aravindram, K. Rohitash, D. V. Gowda, K. Parjanya, *Der Pharmacia. Sinica.* **2012**, *3*, 699–707. **DOI:** www.imedpub.com
- 39. G. M. Lampman, D. L. Pavia, G. S. Kriz, J. R. Vyvyan, A Book for Spectroscopy, 4th International Edition, Brooks/Cole, a part of Cengage Learning India Private Limited, Delhi, India, **2014**, pp. 15–104.
- 40. M. K. Chourasia, L. Kang, S. Y. Chan, *Results Pharma. Sci.* **2011**, *1*, 60–67. **DOI:**10.1016/j.rinphs.2011.10.002
- P. Verma, K. Pathak, *Nanomed*, 2012, 8, 489–496.
 DOI:10.1016/j.nano.2011.07.004
- G. Nethra Vani, M. Alagusundaram, K. B. Chandra Sekhar, Bull. Pharm. Sci. Assiut. Univer. 2022, 45, 507–516.
 DOI:10.21608/bfsa.2022.271485
- 43. D. M. Godbole, P. M. Sabale, V. B. Mathur, *J. Microencap.* **2020**, *37*, 431–444. **DOI**:10.1080/02652048.2020.1778806
- 44. S. M. Honmane, M. S. Charde, R. A. Osmani, *Acta Chim. Slov.* **2023**, *70*, 204–217. **DOI:**10.17344/acsi.2023.8002
- 45. D. S. Gaikwad, R. D. Chougale, K. S. Patil, J. I. Disouza, A. A. Hajare, *Fut. J. Pharma. Sci.* **2023**, *9*, 1–13. **DOI:**10.1186/s43094-023-00494-0
- L. Chin-Chung, Y. Li-Tain, L. Trong, L. David, Y. N. Johnson, *Antimicrob. Age. Chemo.* 2003, 47, 1395–1398 DOI:10.1128/AAC.47.4.1395-1398.2003
- 47. G. Derek, L. Zhiwei, C. Appavu, E. Shaaban, *Pest. Manag. Sci.* **2015**, *71*, 835–841. **DOI**:10.1002/ps.3883
- 48. B. N. Anroop, S. Chaudhary, H. Shah, S. Jacob, V. Mewada, P. Shinu, B. Aldhubiab, *Gels.* **2022**, *8*, 01–24. **DOI:**10.3390/gels8060342
- H. Kadry, B. Noorani, L. Cucullo, Fluids Barri. CNS. 2020, 17,
 DOI:10.1186/s12987-020-00230-3
- H. Udenaes, M. Paalzow, L. K. Lange, *Pharm. Res.* 1997, 14, 128–134. DOI:10.1023/A:1012080106490
- M. D. Shadab, M. Gulam, B. Sanjula, J. Ali, *Drug. Dev. Ind. Pharm.* 2015, 41, 1922–1934.

DOI:10.3109/03639045.2015.1052081

Povzetek

Zdravljenje gliomov ostaja zahtevna naloga. Karmustin je zdravilo, ki se uporablja pri zdravljenju gliomov. Fleksibilne liposome, vgrajene v *in situ* termoreverzibilen nazalni gel, so proučevali z vidika sproščanje karmustina *in vitro*, permeacije karmustina *ex vivo* in kinetike sproščanja karmustina. Med histološko analizo so ugotovili, da so epitelne plasti nosnega tkiva intaktne in nepoškodovane. Intranazalna aplikacija optimiziranih fleksibilnih liposomov, vgrajenih v nazalni gel, je v primerjavi z intravensko aplikacijo karmustina pokazala višje C_{max} (približno dvakrat), $AUC_{0\rightarrow\infty}$ (približno šestkrat) in nižji T_{max} (1 h) v možganih. Pričujoča študija dokazuje, da je termoreverzibilni intranazalni gel karmustina s fleksibilnimi liposomi izboljšal ciljno absorpcijo karmustina v možganih prek nazalnega dostavnega sistema in bi lahko predstavljal zanesljiv in učinkovit dostavni sistem za karmustin pri zdravljenju gliomov.



Except when otherwise noted, articles in this journal are published under the terms and conditions of the Creative Commons Attribution 4.0 International License